HHS Public Access

Author manuscript

J Mol Cell Cardiol. Author manuscript; available in PMC 2023 January 01.

Published in final edited form as:

J Mol Cell Cardiol. 2022 January ; 162: 72–80. doi:10.1016/j.yjmcc.2021.09.005.

Smooth muscle cell CYB5R3 preserves cardiac and vascular function under chronic hypoxic stress

Brittany G. Durgin, Ph.D.[1], **Katherine C. Wood, Ph.D.**[1], **Scott A. Hahn, M.S.**[1], **Brenda McMahon**[1], **Jeffrey J. Baust**[1], **Adam C. Straub, Ph.D.**[1,2,3]

[1]Heart, Lung, Blood and Vascular Medicine Institute, University of Pittsburgh, Pittsburgh, Pennsylvania

[2]Department of Pharmacology and Chemical Biology, University of Pittsburgh, Pittsburgh, Pennsylvania

[3]Center for Microvascular Research, University of Pittsburgh, Pittsburgh, Pennsylvania

Abstract

Chronic hypoxia is a major driver of cardiovascular complications, including heart failure. The nitric oxide (NO) – soluble guanylyl cyclase (sGC) – cyclic guanosine monophosphate (cGMP) pathway is integral to vascular tone maintenance. Specifically, NO binds its receptor sGC within vascular smooth muscle cells (SMC) in its reduced heme (Fe^{2+}) form to increase intracellular cGMP production, activate protein kinase G (PKG) signaling, and induce vessel relaxation. Under chronic hypoxia, oxidative stress drives oxidation of sGC heme ($Fe^{2+}\rightarrow Fe^{3+}$), rendering it NO-insensitive. We previously showed that cytochrome b5 reductase 3 (CYB5R3) in SMC is a sGC reductase important for maintaining NO-dependent vasodilation and conferring resilience to systemic hypertension and sickle cell disease-associated pulmonary hypertension. To test whether CYB5R3 may be protective in the context of chronic hypoxia, we subjected SMC-specific CYB5R3 knockout mice (SMC CYB5R3 KO) to 3 weeks hypoxia and assessed vascular and cardiac function using echocardiography, pressure volume loops and wire myography. Hypoxic stress caused 1) biventricular hypertrophy in both WT and SMC CYB5R3 KO, but to a larger degree in KO mice, 2) blunted vasodilation to NO-dependent activation of sGC in coronary and pulmonary arteries of KO mice, and 3) decreased, albeit still normal, cardiac function in KO mice. Overall, these data indicate that SMC CYB5R3 deficiency potentiates bilateral ventricular hypertrophy and blunts NO-dependent vasodilation under chronic hypoxia conditions. This implicates that SMC CYB5R3 KO mice post 3-week hypoxia have early stages of cardiac remodeling and functional changes that could foretell significantly impaired cardiac function with longer exposure to hypoxia.

Address correspondence to: Adam C. Straub, Ph.D., Associate Professor, Department of Pharmacology and Chemical Biology, University of Pittsburgh School of Medicine, The Heart, Lung, Blood and Vascular Medicine Institute, E1254 Biomedical Science Tower, 200 Lothrop St., Pittsburgh, PA 15216, Tel: 412-648-7097, Fax: 412-648-5980, astraub@pitt.edu.

Keywords

smooth muscle cell; redox; hypoxia; nitric oxide; hypertrophy; soluble guanylyl cyclase

1. Introduction

Chronic hypoxia exposure is a significant risk factor for development of cardiopulmonary diseases leading to pulmonary vasoconstriction and detrimental cardiac remodeling[1–3]. The nitric oxide (NO) – soluble guanylyl cyclase (sGC) – cyclic guanosine monophosphate (cGMP) signaling cascade is a major pathway involved in maintaining vascular tone[4–6]. Specifically, NO produced by endothelial cells diffuses to vascular smooth muscle cells (SMC), where it binds sGC in its reduced heme state to induce cGMP production, protein kinase G (PKG) activation, and vasodilation[5, 7–12]. Chronic hypoxia exposure can result in increased generation of oxidative stress[1–3], which can drive sGC heme oxidation and loss of the sGC heme (apo-sGC)[4, 5, 13]. This results in impaired NO-sGC binding as well as decreased cGMP production and vasoconstriction[4, 5, 13]. To combat this, two new types of sGC therapeutic compounds were developed to enhance cGMP production: sGC stimulators, which target the NO-sensitive reduced sGC heme state, and sGC activators, which act on the NO-insensitive oxidized and apo-sGC heme states[14–16]. Specifically, sGC stimulator compounds work in concert with bioavailable NO to target the NO-sensitive reduced heme form of sGC, resulting in increased cGMP production and restoration of vasodilation[4, 14–16]. Of clinical relevance, sGC stimulators Riociguat and Vericiguat have been shown to have therapeutic efficacy in patients with pulmonary hypertension and heart failure with reduced ejection fraction, respectively[14, 17–19]; both are chronic hypoxia conditions. Therefore, maintaining NO-sGC-cGMP signaling is an important therapeutic avenue for combating chronic hypoxia-induced cardiovascular dysfunction.

Growing evidence suggests that cytochrome b5 reductase 3 (CYB5R3) acts as a sGC reductase ($Fe^{3+}\rightarrow Fe^{2+}$) to maintain the sGC heme iron in its NO-sensitive reduced heme (Fe^{2+}) state[20]. Indeed, CYB5R3, specifically in SMC, has been shown to provide resilience to the development of angiotensin-II induced systemic hypertension[21]. In a Townes sickle-cell disease mouse model, SMC-specific loss of CYB5R3 also resulted in accelerated development of pulmonary hypertension, indicated by an increased right ventricular maximum pressure, right ventricle per tibia area, and left ventricle plus septum per tibia area, compared to wild-type controls[22]. Combined, these previous results demonstrate that SMC-derived CYB5R3 likely provides resilience to the development of systemic hypertension and sickle cell-associated pulmonary hypertension, in part, through its action as a sGC reductase[20–22].

Based on this evidence, we hypothesized that SMC CYB5R3 preserves NOdependent, sGC-mediated vasodilation, conferring protection from chronic hypoxic stress-induced pulmonary and cardiac dysfunction. To test this hypothesis, we subjected tamoxifen-inducible, SMC-specific CYB5R3 knockout mice (SMC CYB5R3 KO) and their wild-type (WT) counterparts to 3 weeks of chronic hypoxia (10% O_2). Surprisingly, we observed that loss of CYB5R3 from SMC resulted in increased left ventricular mass compared

to WT mice. Additionally, chronic hypoxia in SMC CYB5R3 KO mice resulted in decreased cardiac ejection fraction and fractional shortening, as well as blunted coronary and pulmonary artery NO-dependent vasodilation compared to WT mice. Combined, these findings indicate that under hypoxic stress loss of SMC CYB5R3 promotes cardiac hypertrophy, diminished cardiac function and impaired NO-dependent vasodilation without any apparent effects on systemic and pulmonary pressure.

2. Results

To test if CYB5R3 in SMC confers protection under chronic hypoxic stress, we used tamoxifen-inducible smooth muscle cell specific CYB5R3 knockout mice (*Cyb5r3*$^{fl/fl}$ *Myh11-CreER*^{T2}, SMC CYB5R3 KO)[21, 22]. Following tamoxifen treatment, we observed ~60% decrease in SMC CYB5R3 protein expression in coronary and pulmonary arteries (Supplemental Figure 1). Next, we assessed whether cardiac function differed between post-tamoxifen treated, baseline WT and SMC CYB5R3 KO mice (Figure 1A). Echocardiography assessment of baseline WT and SMC CYB5R3 KO mice revealed no differences in either left or right heart function between groups (Figure 1B and Supplemental Tables 1 and 2). Next, baseline WT and SMC CYB5R3 KO mice were placed in hypoxia chambers (10% O2) for 3 weeks (Figure 1A) to induce chronic hypoxic stress. Surprisingly, echocardiography analysis of chronic hypoxia treated WT and SMC CYB5R3 KO mice revealed that SMC CYB5R3 KO mice have a significantly increased left ventricle mass (LV), LV posterior wall thickness at end-diastole (LVPW; d), and LV anterior wall thickness at end-diastole (LVAW; d) compared to WT mice (Figures 1B–D and Supplemental Table 2). SMC CYB5R3 KO mice also had significantly diminished LV ejection fraction compared to WT mice under hypoxic conditions (Figure 1E). These data indicate chronic hypoxic stress leads to a decline in left ventricular function as a result of loss of SMC CYB5R3.

In our assessment of right heart function after 3-weeks of hypoxia, we found no significant differences between WT and SMC CYB5R3 KO mice (Supplemental Table 1). However, 3 week hypoxia treated SMC CYB5R3 KO mice had significantly increased right ventricular internal diameter (RVID) and right ventricular free wall (RVFW) thickness, and decreased pulmonary acceleration time (PAT) and RV fractional area change (FAC) compared to their pre-hypoxia baseline measurements indicative of hypoxia-induced RV remodeling (Supplemental Table 1). In 3-week hypoxia challenged WT mice the tricuspid valve inflow velocity during atrial contraction (TV A) was decreased relative to baseline. However, the more clinically and physiologically relevant TV E/A ratio was not significantly changed, suggesting that RV diastolic function was not affected by hypoxia relative to baseline. Furthermore, WT and SMC CYB5R3 KO mice showed similar increased TV E/A ratio, decreased PAT, and increased RVFW responses to chronic hypoxia when compared to their respective baselines. (Supplemental Table 1). While the PAT decrease in both groups indicates development of increased hypoxia-induced pulmonary pressure, the data overall suggest that RV diastolic function was unchanged by hypoxia irrespective of SMC CYB5R3 availability.

We next performed a gross morphological assessment of hearts from chronic hypoxia-treated WT and SMC CYB5R3 KO mice. Chronic hypoxia treatment resulted in SMC CYB5R3

KO mice having significantly larger left and right ventricle weights normalized to tibia length as compared to WT (Figures 2A and Supplemental Table 3). In addition, while both SMC CYB5R3 KO and WT mice displayed an abnormally high Fulton index in response to chronic hypoxia, which is indicative of RV hypertrophy, the significantly larger Fulton index in SMC CYB5R3 KO mice relative to WT suggests that loss of SMC CYB5R3 actually potentiates RV hypertrophy (Figure 2B). WT and SMC CYB5R3 KO cardiac sections were then assessed for fibrosis by trichrome staining and cardiomyocyte diameter was quantified (Figure 2C). We found that chronic hypoxia did not lead to any significant differences in perivascular or overall cardiac fibrosis in the left or right ventricles of either group (Figure 2D–E). Furthermore, left, but not the right, ventricular cardiomyocytes had significantly larger diameters in SMC CYB5R3 KO mice compared to WT (Figure 2F). Lastly, we performed wheat germ agglutinin staining to assess cardiomyocyte cross-sectional area and found a significant increase for the left, but not right ventricle cardiomyocytes of SMC CYB5R3 KO mice compared to WT (Figure 2G–H). Combined, these data indicate that, under chronic hypoxic stress, the loss of SMC CYB5R3 contributes to biventricular hypertrophy. However, there are likely different mechanisms at work in each ventricle since cardiomyocyte hypertrophy was detected only in the LV.

To determine whether the diminished left heart function observed with SMC CYB5R3 KO was the consequence of change in systemic blood pressure, we performed left ventricle cardiac catheterization in WT and SMC CYB5R3 KO mice after exposure to 3 weeks of hypoxia. We found no significant differences in heart rate, cardiac contractile index, systolic blood pressure (as determined by LV end systolic pressure), or intracardiac pressure in the left ventricle between groups (Figure 3A–D). In addition, no differences in Tau, ventricular end systolic elastance, arterial elastance, or ventricular arterial coupling were seen between WT and SMC CYB5R3 KO mice for the left ventricle (Figure 3E–H). Right ventricle catheterization also showed no differences between chronic hypoxia treated WT and SMC CYB5R3 KO for any of these indices (Figure 3A–H). Taken together, these data indicate that while loss of SMC CYB5R3 in chronic hypoxia conditions resulted in increased left ventricular cardiac hypertrophy, it did not significantly impact upon LV or RV contractility or ventricular-arterial coupling.

In addition to characterizing the cardiac function and morphology, we performed a global assessment of WT and SMC CYB5R3 KO mice to determine if any other organ systems were affected by SMC CYB5R3 KO. Given CYB5R3 is also known as methemoglobin reductase [23, 24], we conducted a complete blood count at baseline and post-3 weeks of hypoxia exposure to further validate the specificity of our SMC CYB5R3 KO and determine if circulating cells differed between groups. The similar red blood cell counts between the KOs and the WT littermates (Supplemental Table 4) suggest that the SMC-CYB5R3 KO was indeed SMC-specific. However, co-oximetry of arterial blood, which was not performed in this study, would be necessary to definitively and directly exclude possible methemoglobinemia that could result from non-specific KO of CYB5R3 in red cells. Lastly, morphologic measurements in hypoxia-stressed animals showed that SMC-CYB5R3 KO did not induce any significant hypertrophy or atrophy of other, non-cardiac, highly vascularized organs (i.e., lungs, liver, spleen, kidney) relative to WT. (Supplemental Table 3).

CYB5R3 has been previously shown to act as a sGC reductase that maintains sGC in its NO-sensitive reduced heme state in response to oxidative stress[20–22]. Therefore, we assessed whether SMC CYB5R3 acts as an sGC reductase in the vasculature in pulmonary and coronary arteries subjected to chronic hypoxic stress. Since it has been reported in cultured SMC that loss of CYB5R3 results in decreased sGCβ levels[20], we quantified total sGCβ protein expression in coronary and pulmonary arteries after chronic hypoxic stress. We found no differences in sGCβ protein expression per artery media area between hypoxia treated WT and SMC CYB5R3 KO mice in either coronary or pulmonary arteries (Figure 4A–D).

We next sought to determine if CYB5R3 in SMC is important for maintenance of sGC heme redox state and NO-mediated vessel function immediately following chronic hypoxia for 3 weeks. To test this, vasodilation was measured in the left anterior descending coronary arteries and second order pulmonary arteries from WT and SMC CYB5R3 KO mice subjected to chronic hypoxia; responses to NO-donor sodium nitroprusside (SNP), the NO-independent sGC activator BAY 58–2667, and acetylcholine (Ach) were assessed (Figure 5A). SNP targets the reduced state of sGC (sGC^{Fe2+}), while BAY 58–2667 acts on the oxidized (sGC^{Fe3+}) and the apo-sGC states to induce NO-independent vasodilation (Figure 5B)[25–27]. Ach, an endothelium-dependent vasodilator, triggers release of NO along with other vasodilators, including prostaglandins, hydrogen peroxide and endothelial-derived hyperpolarizing factor[28, 29]. In pulmonary arteries, SMC CYB5R3 KO mice showed a significantly impaired vasodilatory response to NO-donor SNP as compared to WT mice (Figure 5C). However, no difference was seen in BAY 58–2667 NO-independent vasodilation between groups (Figure 5D). Similarly, coronary arteries from SMC CYB5R3 KO mice showed a significantly decreased responsiveness to SNP-induced vasodilation but no difference in BAY 58–2667 vasodilation compared to WT mice (Figure 5E–F). In coronary arteries, we found SMC CYB5R3 KO mice had significantly improved Ach-induced vasodilation compared to WT mice (n=7) (Figure 5G). Taken together, these data show that under chronic hypoxic stress, SMC-derived CYB5R3 is important for regulating coronary and pulmonary artery NO-dependent sGC-mediated vasodilation.

The data presented herein indicate that following chronic hypoxic stress, SMC-CYB5R3 deficiency led to potentiated structural remodeling of the heart. Pro-hypertrophic effects of SMC CYB5R3 deficiency differed between the ventricles, with cardiomyocyte hypertrophy occurring in the LV but not RV. Despite relative decrements in echocardiographic measurements of LV and RV function in chronically hypoxic SMC CYB5R3 KO mice relative to baseline, SMC CYB5R3 KO cardiac function (as measured by LVEF and RV FAC) remained within normal limits. Furthermore, PV loop analysis confirmed that cardiac contractility and ventricular-arterial coupling of SMC CYB5R3 KO mice was no different than that of WT mice, following chronic hypoxia. It is possible that loss of SMC CYB5R3 negatively impacts cardiac function at least partially, while other compensatory mechanisms maintain overall normal cardiac function. A limitation of this study is the lack of baseline (normoxic) PV loop analysis data in both WT and SMC CYB5R3 KO mice, which are planned for in future studies. Without these data, it is difficult to definitively determine whether SMC CYB5R3 deficiency compromises the cardiac contractile/functional remodeling response to chronic hypoxic stress.

3. Materials and Methods

3.1 Experimental Animals and Treatment

We have previously detailed generation of tamoxifen-inducible SMC specific CYB5R3 floxed mice (*Cyb5r3*$^{fl/fl}$*Myh11*-CreER^{T2})[21, 22]. Between 14–22 weeks of age, both male SMC CYB5R3 KO mice and their male WT controls (*Cyb5r3*$^{wtl/wt}$*Myh11*-CreER^{T2}) were injected with 1mg per day of tamoxifen for 10 days to induce SMC-specific knockout of CYB5R3 (*Cyb5r3*$^{\Delta/\Delta}$*Myh11*-CreER^{T2}, SMC CYB5R3 KO)[21, 22]. These baseline WT and SMC CYB5R3 KO mice were then placed in 10% O_2 hypoxia chambers for 3 weeks and cardiac and pulmonary endpoints analyzed.

3.2 Echocardiography

The University of Pittsburgh Small Animal Ultrasonography Core performed echocardiogram measurements and analysis. Mice were anesthetized with 3% isoflurane and placed on a 37°C heat pad to maintain body temperature. During image acquisitions, isoflurane anesthetization was maintained at 1–2% to maintain a heart rate between 400–500 beats per minute (bpm). Cardiac images were acquired with a Vevo 3100 imaging system and VisualSonic MX400 (20–46 MHz, 50 μm axial resolution) linear array transducer (FUJIFILM, VisualSonics, Toronto, Canada). The RVIDd was measured in the right parasternal long axis image with m-mode imaging.

3.3 Complete Blood Count Measurements

Retroorbital blood was collected from mice post-tamoxifen injection with mice anesthetized briefly (<5 minutes) by 1% isoflurane. After 3 weeks hypoxia, blood was collected via cardiac puncture from mice anesthetized with etomidate/urethane (9/1.1mg/kg intraperitoneally). Coagulation was prevented in blood samples by adding EDTA when collected and blood counts analyzed using a HemaTrue machine (Heska Inc). For complete blood count measurements, blood was drawn from the same group of mice at post-tamoxifen baseline and at 3 weeks of hypoxia. Therefore, comparisons between baseline versus chronic hypoxia within the same genotype were assessed for normality by Shapiro-Wilk normality test and then either subjected to paired two tailed *t*-test analysis (p) if data were normally distributed or subjected to a Wilcoxon matched-pairs signed rank test (*p) if data were not normally distributed.

3.4 Hemodynamic and Ventricular Micro-Catheterization

Experiments were performed by the University of Pittsburgh Small Rodent Core. Mice were anesthetized with etomidate/urethane (9/1.1mg/kg, Butler Schein) and placed on a 37°C heating pad to regulate body temperature. The mouse neck muscles were carefully resected to expose an approximately 20 millimeter section of the jugular vein and then intubated to assist with breathing. Two 6–0 silk surgical sutures were placed on the jugular vein: one tightly placed at the cranial end of the jugular vein and another lightly looped closer to the heart. A small incision was then made and a 1.2F micro pressure-volume (PV) catheter was threaded into the jugular, followed by the suture near the heart on the jugular vein tightened to prevent bleeding, and finally guidance of the catheter to the right side of the heart.

After 5 minutes of catheter stabilization in the right heart, pressure measurements were recorded. For left ventricular measurements, mice were similarly anesthetized and intubated. However, the chest cavity was opened and the catheter was threaded into the left ventricle at the apex of the heart. After 5 minutes of catheter stabilization in the left heart, pressure measurements were recorded. Analysis of the recordings was performed on IOX2 software (EMKA Technologies). Mean pulmonary artery pressure (calculated) = SBP * 0.65 + 0.55 mmHg, with RV pressure max substituted for SBP, as described in Syyed et al.[30]

3.5 Trichrome Analysis of Fibrosis

Trichrome analysis was conducted as described previously[21]. Cardiac tissue sections were stained with Masson's Trichrome Kit (Thermo Fisher Scientific, 87019) using the manufacturer's protocol to assess fibrosis. Tissue sections were imaged via Tissuegnostics Microscope at 20x objective and stitched together using Nikon Elements Software using 8% overlap. In Fiji software, a threshold was set to identify fibrosis and was applied to each image. The images were converted to a binary image format from the threshold and quantified. Total tissue area was quantified in the same manner with a threshold set for total tissue and total fibrosis per tissue area reported. To assess perivascular fibrosis, a region of interest was drawn around the arterial media of a single coronary artery selected in the left and right ventricle. A second region of interest was drawn around the blue colored matrix staining for collagen surrounding the vessel, indicative of perivascular fibrosis, to the point where the blue came in contact with cardiomyocytes (pink). The ratio of perivascular fibrosis normalized to artery medial area is reported. For cardiomyocyte diameter measurements, the length of 10 cardiomyocytes randomly selected near a coronary artery were averaged and compared between groups.

3.6 Immunofluorescence Analysis

Immunofluorescence analysis was done as described previously[21]. Mouse tissues were fixed in 4% paraformaldehyde (Santa Cruz, sc-281692) for 24 hours, placed in 70% ethanol, processed, paraffin-embedded, and sectioned. Tissue sections were deparaffinized, rehydrated in distilled H_2O, and subjected to heat-mediated citric acid-based antigen retrieval (Vector Laboratories, H-3300) for 20 minutes then cooled. Sections were then incubated in PBS with 10% horse serum (Sigma, H1138–100) for 1 hour at room temperature. Primary antibody incubation in PBS containing 10% horse serum was then done overnight at 4°C in a humidity chamber with the following antibodies: CYB5R3 (Proteintech, 10894–1-AP, 1:100) or sGCβ (Cayman Chemical, 160897, 1:100), and Von Willebrand Factor (VWF - Abcam, ab11713, 1:250). One section per slide was stained with a rabbit IgG control (Vector Laboratories, I-1000) that matched in concentration and dilution that of CYB5R3 and sGCβ respectively as a negative control. Slides were washed then incubated with the following secondary antibodies diluted in PBS with 10% horse for 1 hour at room temperature: smooth muscle α-actin-FITC (ACTA2-FITC - MilliporeSigma, F3777 clone 1A4, 1:500), donkey anti-rabbit 594 (Invitrogen, A-21207, 1:250), DAPI (Thermo Fisher Scientific, D3571, 1:100), and donkey anti-sheep 647 (Invitrogen, A-21448, 1:250). Slides were then washed and cover-slipped with Prolong Gold Antifade with DAPI reagent (Invitrogen, P36931). Z-stack images of arteries were taken with a Nikon A1 Confocal Laser Microscope at the Center for Biological Imaging at the University of Pittsburgh at

40x magnification, 1096 × 1096 resolution, and at 1 μm increments. Maximum intensity images were created in Nikon Elements Software. Regions of interest were drawn in the maximum intensity projections in Fiji software for ACTA2+ areas indicative of SMC media and superimposed on the corresponding sGCβ or CYB5R3 images. The raw integrated intensity per media area was then quantified and reported.

For wheat germ agglutinin staining, cardiac sections were deparaffinized, underwent heat-mediated antigen retrieval, and subsequently incubated in PBS with 10% horse serum for 1 hour at room temperature. Cardiac sections were then incubated in PBS with 10% horse serum containing antibodies for wheat germ agglutinin (WGA) conjugated to Alexa Fluor 488 (Invitrogen, W11261) and DAPI (as stated above) for 30 minutes at room temperature. Slides were then washed thrice in PBS and cover-slipped with Prolong Gold Antifade with DAPI reagent. Coronary arteries were located within cardiac sections and a single plane image taken with a Nikon A1 Confocal Laser Microscope at the Center for Biological Imaging at the University of Pittsburgh at 40x magnification and 1096 × 1096 resolution. In ImageJ, the cross-sectional area of 10 randomly sampled cardiomyocytes surrounding coronary arteries were quantified and averaged per mouse. Subsequently, the cross-sectional area of cardiomyocytes per genotype was compared and reported.

3.7 Wire myography

Murine lungs and hearts were rapidly excised and placed in room temperature physiological salt solution (PSS) as described previously[21]. The second order pulmonary arteries and left anterior descending coronary arteries were cleaned of tissue and cut into 2 millimeter rings. Two wires that were 25 microns in diameter were threaded through the lumen and placed on a small vessel wire myograph (DMT 620M) filled with PSS at 37°C. Following a 30-minute rest, arteries were gradually stretched to a tension corresponding to a transmural pressure of 80mmHg. Viability was tested by 60mM KCl exposure for 5 minutes. Rings were washed thrice with PSS and rested for another 30 minutes. PSS was replaced and vessels rested for an additional 10 minutes. Next, coronary and pulmonary arteries were constricted with cumulative doses of phenylephrine (10^{-6} – 10^{-5} M) or prostaglandin F2 ($PGF_{2\alpha}$, 10^{-7} – 10^{-5} M, Tocris #4214), respectively, at 4-minute intervals until the vessels reached ~50% vasoconstriction. Vessel were then treated with cumulative doses of NO-donor sodium nitroprusside (SNP, 10^{-9} – 10^{-4} M, Sigma-Aldrich, #71778) at 3-minute intervals, acetylcholine at 3-minute intervals (Ach, 10^{-8} – 10^{-5} M, Sigma Aldrich, #A6625), or NO-independent vasodilator BAY 58–2667 (10^{-12} – 10^{-6} M, Bayer AG Pharmaceuticals) at 5-minute intervals. Lastly, vessels were treated with Ca^{2+}-free PSS containing 100μM SNP to determine maximal vessel dilation. Vessel reactivity was normalized to the change in maximal constriction with $PGF_{2\alpha}$ or phenylephrine to maximal dilation from Ca^{2+}-free PSS with 100 μM SNP to determine the percent relaxation reported herein.

3.8 Statistical Analysis

All data analysis was done using Graphpad Prism Software version 7.0d. Data was assessed for normality using Shapiro-Wilk normality test. If data was normally distributed, unpaired two-tailed *t*-tests were performed. If data was normally distributed but was found by F-test to have unequal variances, unpaired two-tailed *t*-test with a Welch's correction was

applied. For data that was not normally distributed, a Mann Whitney *U* test was used. For wire myography experiments, two way-ANOVA analyses with post-hoc Sidak's multiple comparisons test were conducted. Figure legends include information for which statistical tests were done for each analysis and n values which indicate the number of mice or samples for each analysis.

4. Discussion

We show for the first time that SMC CYB5R3 is important in preserving cardiac function and pulmonary vasodilation when challenged by chronic hypoxia. This work builds upon previous lines of evidence showing that SMC derived CYB5R3 plays a significant and protective role in cardiovascular and pulmonary disease. Both prior[21] and current evidence herein show that SMC CYB5R3 KO mice exhibited a blunted NO-dependent vasodilation response in the context of oxidative stress, implicating a major function of CYB5R3 in SMC as a sGC heme iron reductase to maintain NO-dependent sGC-mediated vasodilation. In sickle cell-associated pulmonary hypertension, loss of SMC CYB5R3 accelerated development of pulmonary hypertension and cardiac hypertrophy[22]. In this study, we observed that chronic hypoxia treatment alone leads to cardiac hypertrophy in mice lacking SMC CYB5R3. While we previously reported SMC CYB5R3 KO mice in normoxic conditions had a slight but significant 5.84-mmHg higher systemic mean arterial pressure[21] relative to WT using telemetry, we found baseline WT and SMC CYB5R3 KO mice in this study did not exhibit any differences in cardiac function. Moreover, chronic hypoxia treated WT and SMC CYB5R3 KO animals had no differences in systemic or pulmonary pressures, further suggesting pressure is likely not a driver of the changes in cardiac function in SMC CYB5R3 KO mice. Instead, evidence suggests that hypoxic conditions are a driver of SMC derived CYB5R3-mediated cardiac dysfunction and hypertrophy[21, 22]. Studies in several different SMC-specific knockout mouse models have shown that SMC-derived proteins are important contributors to the regulation of cardiac function in the context of chronic hypoxia, though this was accompanied by changes in either pulmonary or systemic pressures[31–33]. Thus, our studies provide the first evidence that under chronic hypoxia conditions, cardiac hypertrophy is seen with loss of SMC CYB5R3.

Notably, the left ventricle of 3 week hypoxia treated SMC CYB5R3 KO mice showed functional impairment and cardiomyocyte hypertrophy compared to WT controls. The decreased left ventricular ejection fraction (LVEF) in the absence of data supportive of less efficient ventricular-arterial coupling (Ees, Ea, LV dP/dt max and systemic blood pressure changes) likely signifies early stages of impairment to LV function, which is still more than 50 percent of normal. As such, the decreased LVEF would still be considered "preserved", as opposed to "reduced," and thus not yet be sufficient to have a detrimental effect on ventricular-arterial coupling (decreased Ees and/or increased Ea) or systemic blood pressure in the hypoxia-treated SMC CYB5R3 KO mice. We predict that increasing the duration of the chronic hypoxia by additional weeks or months may be necessary for the decrease in LVEF to reach a level that produces more systemic cardiovascular effects.

With respect to the right ventricle, we detected no differences in RV function between hypoxic WT and SMC CYB5R3 KO mice by echocardiography, nor via histological measurements of fibrosis and cardiomyocyte hypertrophy. However, we found that SMC CYB5R3 KO mice subjected to hypoxia had an increased Fulton index compared to similarly treated WT mice. It is important to note that the Fulton index was determined by comparing weights of the right ventricle with the left ventricle plus septum in freshly isolated hearts that contain interstitial fluid. In order to perform histological analyses, these hearts were immediately placed post-weighing in paraformaldehyde, then subsequently stored in 70% ethanol, before being processed for paraffin embedding. Given the ethanol and processing for paraffin embedding dehydrates the tissue, we were not able to assess interstitial fluid accumulation in the heart from a potentially leaky cardiac vasculature in our histological assessments. Prospective studies to address possible interstitial fluid accumulation by assessing nonfixed ventricular tissue or use of cardiac magnetic resonance imaging would be needed to confirm this concept.

Contrary to previous studies[20–22], the sGC activator BAY 58–2667 did not enhance *ex vivo* vasodilation in SMC CYB5R3 KO pulmonary and coronary arteries isolated from animals subjected to chronic hypoxia. In cultured rat aortic vascular SMC, CYB5R3 knockdown has been shown to decrease sGCβ levels[20]. However, chronic hypoxic stress elicited no differences in sGCβ protein expression between WT and SMC CYB5R3 KO vessels (Figure 4). Moreover, both WT and SMC CYB5R3 KO isolated pulmonary and coronary arteries from mice exposed to chronic hypoxia respond to BAY 58–2667 indicating it is also unlikely that there is differential phosphodiesterase-mediated cGMP degradation occurring between groups[34–36]. Nonetheless, we cannot rule out the potential possibility for differential subcellular localization of sGC-cGMP and co-compartmentalization with phosphodiesterase 5 (PDE5) in our studies[25, 37–39]. It is important to note that BAY 58–2667 has been shown to bind to the heme pocket of apo-sGC[5, 27]. However, a definitive understanding of the key mechanisms and proteins involved in the transition from oxidized to heme-deficient apo-sGC remain largely unknown. Purified enzyme studies have shown that in anaerobic conditions, increasing NO concentrations lead to an increase in reductive S-nitrosation of the cysteine residues on the oxidized ferric, but not the reduced ferrous form of sGCβ[40]. It is likely that loss of CYB5R3 leads to increased ferric sGC formation, which may enhance reductive S-nitrosation of sGC, thereby limiting sGC activity. In addition, it is possible that S-nitrosation aids to “lock in” the heme to its binding site, rendering it unable to be activated by BAY 58–2667. Indeed, work by *Kirsch et al* has shown that with 21-days of chronic hypoxia, conditions near identical to those herein, there was an increase in nitric oxide synthase (NOS) 2 and 3, a decrease in phosphodiesterase 5 (PDE5), but no change in sGCβ protein levels in the lung compared to normoxic control lungs[35]. In addition, BAY 58–2667 treatment between days 21–35 of chronic hypoxia failed to reverse right ventricular systolic pressure changes or right heart hypertrophy in global NOS3 knockout mice suggesting there may be a NOS3-dependent function for BAY 58–2667[41]. Taken together, we therefore propose the concept that in low oxygen there may be a stabilization of the oxidized form of sGC through an as yet unknown and unproven physiological mechanism; we hypothesize perhaps through S-nitrosation of sGC cysteine residues. Thus, while loss of SMC CYB5R3 would, in theory, increase the rate and/or quantity of generation

of oxidized heme sGC and the S-nitrosation, the WT and SMC CYB5R3 KO in chronic hypoxia would have similar levels of apo-sGC and similar BAY 58–2667 response.

Although we observed reduced NO-mediated vasodilation and no change in BAY 58–2667 vasodilation in the coronary arteries, we did observe a significant improvement in acetylcholine-mediated vasodilation in coronary arteries. These results may explain why we observed no difference in either pulmonary or systemic blood pressure. It is well known that acetylcholine can trigger the release of several vasodilators besides NO, including prostaglandins, hydrogen peroxide and endothelial-derived hyperpolarizing factors in the coronary circulation to cause a shift in vasodilator response under various pathophysiological conditions[28, 29]. These results may infer that SMC CYB5R3 can facilitate an endothelium-dependent “vasodilator switch” under hypoxic conditions to preserve endothelium-dependent vasodilation and preserve coronary blood flow. Future studies are needed to explore this idea.

Mechanistically, our data may suggest that there is a disruption in SMC-cardiomyocyte cross-talk in the setting of chronic hypoxic stress in SMC CYB5R3 KO mice that is absent in WT controls. Of note, earlier work by *Krawutschke et al.* has shown that cGMP generated in SMC can be transferred out of SMC by ABC transporter multidrug resistance-associated protein 4 (MRP4)[42, 43]. Work by *Menges et al* has shown in an *in vitro* co-culture model that NO-induced cGMP production in cardiac fibroblasts can traverse gap junctions and accumulate in cardiomyocytes[44]. Increased cardiac myocyte cGMP has been associated with decreased cardiac hypertrophy[25]. Given our data herein, it stands to reason that NO-sGC-cGMP activation and regulation of sGC redox state, in part by CYB5R3, in the coronary circulation may be a crucial protective mechanism for preventing cardiomyocyte hypertrophy and possible heart failure. An intriguing hypothesis to explore will be if SMC-cardiomyocyte cross-talk might include the transfer of cGMP via gap junctions and to test definitively if CYB5R3 may influence this process.

As shown in our data, CYB5R3 acts as a sGC heme reductase to preserve NO-dependent vasodilation and is protective against left ventricular cardiac dysfunction under chronic hypoxic stress. Notably, sGC stimulator therapy Riociguat, which works in concert with bioavailable NO to improve NO-dependent sGC activity and cGMP production, has been tested clinically in patients with pulmonary hypertension and either left ventricular dysfunction or diastolic heart failure. In both the Left Ventricular Systolic Dysfunction Associated with Pulmonary Hypertension Riociguat Trial (LEPHT) and the Acute Hemodynamic Effects of Riociguat in Patients with Pulmonary Hypertension Associated with Diastolic Heart Failure (DILATE-1) trials, patients exhibited significant improvement in cardiac index and stroke volume[45–47]. Future translational studies assessing whether sGC stimulator treatment in our SMC CYB5R3 KO mice subjected to chronic hypoxia may prevent or even reverse the cardiac dysfunction are needed. Of additional clinical relevance, a CYB5R3 loss of function mutation rs1800457, which substitutes a serine for a threonine (T117S), is found at an allelic frequency of 0.23 in those of African descent[48, 49]. A pertinent planned direction of exploration will be to assess whether CYB5R3 variants, particularly this T117S loss of function variant, may serve as a biomarker to identify patients with more severe cardiopulmonary disease.

5. Conclusion

Our studies are the first to show that CYB5R3 expression in vascular smooth muscle cells is important for maintaining cardiac function and NO-dependent vasodilation in response to chronic hypoxic stress.

Supplementary Material

Refer to Web version on PubMed Central for supplementary material.

Acknowledgments

We would like to acknowledge the Small Animal Hemodynamics Core, Small Animal Ultrasonography Core, and Animal Phenotyping Facility at the Heart, Lung, Blood and Vascular Medicine Institute at the University of Pittsburgh for their assistance in phenotyping our mice. We also would like to acknowledge Michele Mulkeen at the Rangos Histology Core lab for processing our tissue samples. We acknowledge the Center for Biological Imaging at the University of Pittsburgh for providing training, access, and support for use of their Tissuegnostics, Nikon A1 Confocal Laser microscope, and Nikon Elements Software. Bayer was kind enough to provide the BAY 58-2667 compound. We would also like to acknowledge the graphical abstract was created with BioRender.com.

Financial support for this work was provided by the National Institutes of Health (NIH) [R01 HL 133864, R01 HL 128304, F32 HL152498-01, DK007052, 1S10OD023684-01A1]; and the American Heart Association (AHA) [16GRNT27250146].

7. Disclosures

A.C.S has received research funds from Bayer AG Pharmaceuticals.

8. References

[1]. Rosenkranz S, Gibbs JS, Wachter R, De Marco T, Vonk-Noordegraaf A, Vachiery JL. Left ventricular heart failure and pulmonary hypertension. Eur Heart J 2016; 37(12): 942–54. [PubMed: 26508169]

[2]. Young JM, Williams DR, Thompson AAR. Thin Air, Thick Vessels: Historical and Current Perspectives on Hypoxic Pulmonary Hypertension. Front Med (Lausanne) 2019; 6: 93. [PubMed: 31119132]

[3]. Abe H, Semba H, Takeda N. The Roles of Hypoxia Signaling in the Pathogenesis of Cardiovascular Diseases. J Atheroscler Thromb 2017; 24(9): 884–894. [PubMed: 28757538]

[4]. Stasch JP, Schmidt P, Alonso-Alija C, Apeler H, Dembowsky K, Haerter M, et al. NO- and haem-independent activation of soluble guanylyl cyclase: molecular basis and cardiovascular implications of a new pharmacological principle. Br J Pharmacol 2002; 136: 773–783. [PubMed: 12086987]

[5]. Stasch JP, Schmidt PM, Nedvetsky PI, Nedvetskaya TY, H. S. A, Meurer S, et al. Targeting the heme-oxidized nitric oxide receptor for selective vasodilatation of diseased blood vessels. J Clin Invest 2006; 116(9): 2552–61. [PubMed: 16955146]

[6]. Thoonen R, Cauwels A, Decaluwe K, Geschka S, Tainsh RE, Delanghe J, et al. Cardiovascular and pharmacological implications of haem-deficient NO-unresponsive soluble guanylate cyclase knock-in mice. Nat Commun 2015; 6: 8482. [PubMed: 26442659]

[7]. Lee YC, Martin E, Murad F. Human recombinant soluble guanylyl cyclase: expression, purification, and regulation. Proc Natl Acad Sci U S A 2000; 97(20): 10763–8. [PubMed: 10995472]

[8]. Zhao Y, Marletta MA. Localization of the heme binding region in soluble guanylate cyclase. Biochemistry 1997; 36(36): 15959–15964. [PubMed: 9398330]

[9]. Karow DS, Pan D, Davis JH, Behrends S, Mathies RA, Marletta MA. Characterization of functional heme domains from soluble guanylate cyclase. Biochemistry 2005; 44(49): 16266–74. [PubMed: 16331987]

[10]. Underbakke ES, Iavarone AT, Marletta MA. Higher-order interactions bridge the nitric oxide receptor and catalytic domains of soluble guanylate cyclase. Proc Natl Acad Sci U S A 2013; 110(17): 6777–82. [PubMed: 23572573]

[11]. Ma X, Sayed N, Baskaran P, Beuve A, van den Akker F. PAS-mediated dimerization of soluble guanylyl cyclase revealed by signal transduction histidine kinase domain crystal structure. J Biol Chem 2008; 283(2): 1167–78. [PubMed: 18006497]

[12]. Rothkegel C, Schmidt PM, Atkins DJ, Hoffmann LS, Schmidt HH, Schroder H, et al. Dimerization region of soluble guanylate cyclase characterized by bimolecular fluorescence complementation in vivo. Mol Pharmacol 2007; 72(5): 1181–90. [PubMed: 17715400]

[13]. Kalk P, Godes M, Relle K, Rothkegel C, Hucke A, Stasch JP, et al. NO-independent activation of soluble guanylate cyclase prevents disease progression in rats with 5/6 nephrectomy. Br J Pharmacol 2006; 148(6): 853–9. [PubMed: 16770325]

[14]. Dasgupta A, Bowman L, D'Arsigny CL, Archer SL. Soluble guanylate cyclase: a new therapeutic target for pulmonary arterial hypertension and chronic thromboembolic pulmonary hypertension. Clin Pharmacol Ther 2015; 97(1): 88–102. [PubMed: 25670386]

[15]. Stasch JP, Pacher P, Evgenov OV. Soluble guanylate cyclase as an emerging therapeutic target in cardiopulmonary disease. Circulation 2011; 123(20): 2263–73. [PubMed: 21606405]

[16]. Sandner P, Zimmer DP, Milne GT, Follmann M, Hobbs A, Stasch JP. Soluble Guanylate Cyclase Stimulators and Activators, Handb Exp Pharmacol. 2019: 1–40. [PubMed: 30430259]

[17]. Ghofrani HA, D'Armini AM, Grimminger F, Hoeper MM, Jansa P, Kim NH, et al. Riociguat for the treatment of chronic thromboembolic pulmonary hypertension. N Engl J Med 2013; 369(4): 319–29. [PubMed: 23883377]

[18]. Ghofrani HA, Galie N, Grimminger F, Grunig E, Humbert M, Jing ZC, et al. Riociguat for the treatment of pulmonary arterial hypertension. N Engl J Med 2013; 369(4): 330–40. [PubMed: 23883378]

[19]. Armstrong PW, Pieske B, Anstrom KJ, Ezekowitz J, Hernandez AF, Butler J, et al. Vericiguat in Patients with Heart Failure and Reduced Ejection Fraction. N Engl J Med 2020; 382(20):1883–1893. [PubMed: 32222134]

[20]. Rahaman MM, Nguyen AT, Miller MP, Hahn SA, Sparacino-Watkins C, Jobbagy S, et al. Cytochrome b5 Reductase 3 Modulates Soluble Guanylate Cyclase Redox State and cGMP Signaling. Circ Res 2017; 121(2):137–148. [PubMed: 28584062]

[21]. Durgin BG, Hahn SA, Schmidt HM, Miller MP, Hafeez N, Mathar I, et al. Loss of smooth muscle CYB5R3 amplifies angiotensin II-induced hypertension by increasing sGC heme oxidation. JCI Insight 2019; 4(19): e129183.

[22]. Wood KC, Durgin BG, Schmidt HM, Hahn SA, Baust JJ, Bachman T, et al. Smooth muscle cytochrome b5 reductase 3 deficiency accelerates pulmonary hypertension development in sickle cell mice. Blood Adv 2019; 3(23): 4104–4116. [PubMed: 31821458]

[23]. Straub AC, Butcher JT, Billaud M, Mutchler SM, Artamonov MV, Nguyen AT, et al. Hemoglobin alpha/eNOS coupling at myoendothelial junctions is required for nitric oxide scavenging during vasoconstriction. Arterioscler Thromb Vasc Biol 2014; 34(12): 2594–600. [PubMed: 25278292]

[24]. Straub AC, Lohman AW, Billaud M, Johnstone SR, Dwyer ST, Lee MY, et al. Endothelial cell expression of haemoglobin alpha regulates nitric oxide signalling. Nature 2012; 491(7424): 473–7. [PubMed: 23123858]

[25]. Tsai EJ, Kass DA. Cyclic GMP signaling in cardiovascular pathophysiology and therapeutics. Pharmacol Ther 2009; 122(3): 216–38. [PubMed: 19306895]

[26]. Kraehling JR, Sessa WC. Contemporary Approaches to Modulating the Nitric Oxide-cGMP Pathway in Cardiovascular Disease. Circ Res 2017; 120(7): 1174–1182. [PubMed: 28360348]

[27]. Surmeli NB, Marletta MA. Insight into the rescue of oxidized soluble guanylate cyclase by the activator cinaciguat. Chembiochem 2012; 13(7): 977–81. [PubMed: 22474005]

[28]. Goodwill AG, Dick GM, Kiel AM, Tune JD. Regulation of Coronary Blood Flow, Compr Physiol 2017; 7(2): 321–382. [PubMed: 28333376]

[29]. Beyer AM, Gutterman DD. Regulation of the human coronary microcirculation. J Mol Cell Cardiol 2012; 52(4): 814–21. [PubMed: 22033434]

[30]. Syyed R, Reeves JT, Welsh D, Raeside D, Johnson MK, Peacock AJ. The relationship between the components of pulmonary artery pressure remains constant under all conditions in both health and disease. Chest 2008; 133(3): 633–9. [PubMed: 17989160]

[31]. Zhang L, Wang Y, Wu G, Rao L, Wei Y, Yue H, et al. Blockade of JAK2 protects mice against hypoxia-induced pulmonary arterial hypertension by repressing pulmonary arterial smooth muscle cell proliferation. Cell Prolif 2020; 53(2): e12742. [PubMed: 31943454]

[32]. Kim YM, Barnes EA, Alvira CM, Ying L, Reddy S, Cornfield DN. Hypoxia-inducible factor-1alpha in pulmonary artery smooth muscle cells lowers vascular tone by decreasing myosin light chain phosphorylation. Circ Res 2013; 112(9): 1230–3. [PubMed: 23513056]

[33]. Luo Y, Teng X, Zhang L, Chen J, Liu Z, Chen X, et al. CD146-HIF-1alpha hypoxic reprogramming drives vascular remodeling and pulmonary arterial hypertension. Nat Commun 2019; 10(1); 3551. [PubMed: 31391533]

[34]. Zhao L, Mason NA, Strange JW, Walker H, Wilkins MR. Beneficial effects of phosphodiesterase 5 inhibition in pulmonary hypertension are influenced by natriuretic peptide activity. Circulation 2003; 107(2): 234–7. [PubMed: 12538421]

[35]. Kirsch M, Kemp-Harper B, Weissmann N, Grimminger F, Schmidt HH. Sildenafil in hypoxic pulmonary hypertension potentiates a compensatory up-regulation of NO-cGMP signaling. FASEB J 2008; 22(1): 30–40. [PubMed: 17679609]

[36]. Zhao L, Mason NA, Morrell NW, Kojonazarov B, Sadykov A, Maripov A, et al. Sildenafil inhibits hypoxia-induced pulmonary hypertension. Circulation 2001; 104: 424–428. [PubMed: 11468204]

[37]. Tsai EJ, Liu Y, Koitabashi N, Bedja D, Danner T, Jasmin JF, et al. Pressure-overload-induced subcellular relocalization/oxidation of soluble guanylyl cyclase in the heart modulates enzyme stimulation. Circ Res 2012; 110(2): 295–303. [PubMed: 22095726]

[38]. Zhang L, Bouadjel K, Manoury B, Vandecasteele G, Fischmeister R, Leblais V. Cyclic nucleotide signalling compartmentation by PDEs in cultured vascular smooth muscle cells. Br J Pharmacol 2019; 176(11): 1780–1792. [PubMed: 30825186]

[39]. Feiteiro J, Verde I, Cairrao E. Cyclic guanosine monophosphate compartmentation in human vascular smooth muscle cells. 2016; Cell Signal 28(3): 109–116. [PubMed: 26689737]

[40]. Fernhoff NB, Derbyshire ER, Underbakke ES, Marletta MA. Heme-assisted S-nitrosation desensitizes ferric soluble guanylate cyclase to nitric oxide. J Biol Chem 2012; 287(51): 43053–62. [PubMed: 23093402]

[41]. Dumitrascu R, Weissmann N, Ghofrani HA, Dony E, Beuerlein K, Schmidt H, et al. Activation of soluble guanylate cyclase reverses experimental pulmonary hypertension and vascular remodeling. Circulation 2006; 113(2): 286–95. [PubMed: 16391154]

[42]. Krawutschke C, Koesling D, Russwurm M. Cyclic GMP in Vascular Relaxation: Export Is of Similar Importance as Degradation. Arterioscler Thromb Vasc Biol 2015; 35(9): 2011–9. [PubMed: 26205960]

[43]. Stangherlin A, Zoccarato A. Relax: It's Not All About Degradation. Arterioscler Thromb Vasc Biol 2015; 35(9): 1907–9. [PubMed: 26310809]

[44]. Menges L, Krawutschke C, Fuchtbauer EM, Fuchtbauer A, Sandner P, Koesling D et al. Mind the gap (junction): cGMP induced by nitric oxide in cardiac myocytes originates from cardiac fibroblasts. Br J Pharmacol 2019; 176(24): 4696–4707. [PubMed: 31423565]

[45]. Bonderman D, Ghio S, Felix SB, Ghofrani HA, Michelakis E, Mitrovic V, et al. Riociguat for patients with pulmonary hypertension caused by systolic left ventricular dysfunction: a phase IIb double-blind, randomized, placebo-controlled, dose-ranging hemodynamic study. Circulation 2013; 128(5): 502–11. [PubMed: 23775260]

[46]. Koress C, Swan K, Kadowitz P. Soluble Guanylate Cyclase Stimulators and Activators: Novel Therapies for Pulmonary Vascular Disease or a Different Method of Increasing cGMP? Curr Hypertens Rep 2016; 18(5): 42. [PubMed: 27118316]

[47]. Bonderman D, Pretsch I, Steringer-Mascherbauer R, Jansa P, Rosenkranz S, Tufaro C, et al. Acute hemodynamic effects of riociguat in patients with pulmonary hypertension associated with

diastolic heart failure (DILATE-1): a randomized, double-blind, placebo-controlled, single-dose study. Chest 2014; 146(5): 1274–1285. [PubMed: 24991733]

[48]. Jenkins MM, Prchal JT. A high-frequency polymorphism of NADH-cytochrome b5 reductase in African-Americans. Hum Genet 1997; 99: 248–250. [PubMed: 9048929]

[49]. Percy MJ, Lappin TR. Recessive congenital methaemoglobinaemia: cytochrome b(5) reductase deficiency. Br J Haematol 2008; 141(3): 298–308. [PubMed: 18318771]

Highlights

- Chronic hypoxia is an underlying cause of pulmonary hypertension and heart failure
- In chronic hypoxia, smooth muscle specific deletion of CYB5R3 increases cardiac hypertrophy
- Smooth muscle cell CYB5R3 is important for maintaining NO-dependent vasodilation under chronic hypoxic stress

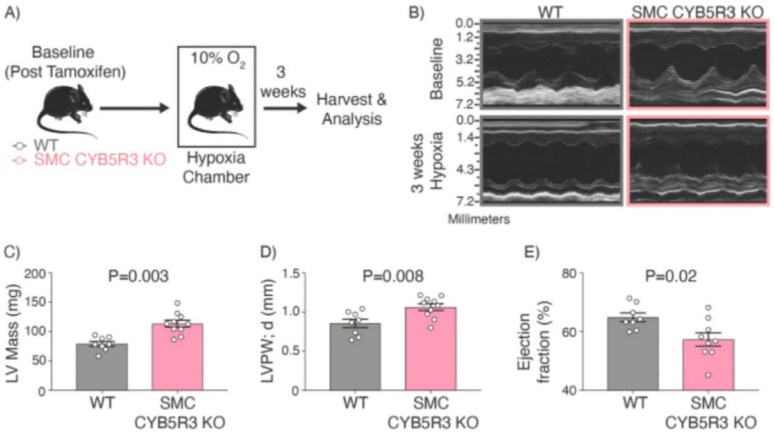

Figure 1: 3 weeks of chronic hypoxia results in SMC CYB5R3 KO mice with increased left ventricular (LV) mass, and decreased LV ejection fraction compared to WT mice.

A) Schematic representation showing baseline (post tamoxifen treated) WT and SMC CYB5R3 KO mice were subjected to hypoxic stress (10% O_2) for 3 weeks. Cardiac and pulmonary physiology was assessed at baseline and post hypoxia. **B-D)** Chronic hypoxia treated SMC CYB5R3 KO mice (n=10) have significantly increased left ventricular wall mass compared to WT mice (n=8). **E)** 3-week hypoxia treated SMC CYB5R3 KO mice (n=9) have significantly decreased ejection fraction as compared to WT mice (n=8). The data represent mean ± standard error of the mean (SEM). P values represent unpaired, two tailed *t*-test comparison between WT and SMC CYB5R3 KO mice.

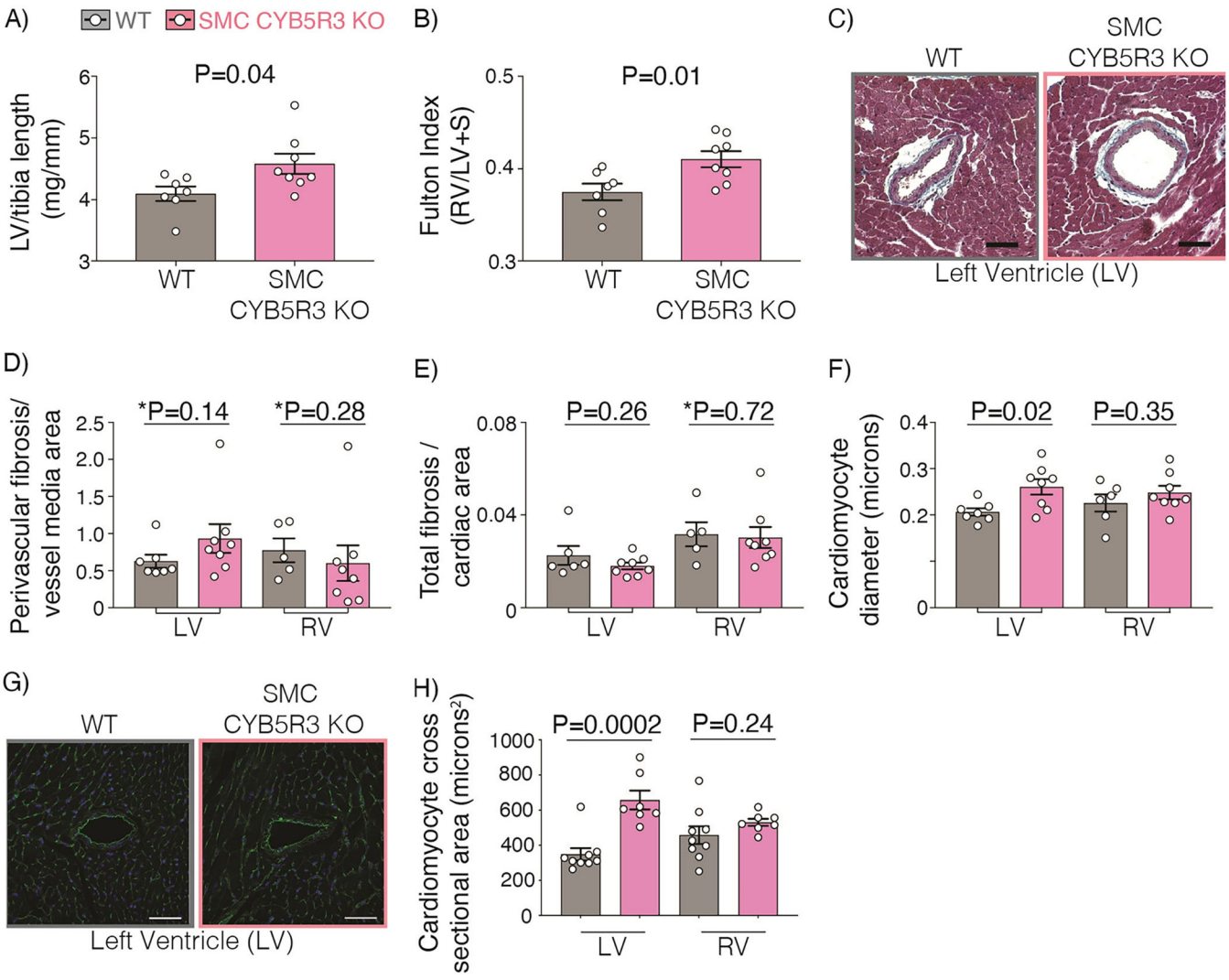

Figure 2: 3 weeks chronic hypoxia results in increased left ventricular (LV) hypertrophy in SMC CYB5R3 KO mice compared to WT but no differences in cardiac fibrosis between groups.

A-B) SMC CYB5R3 KO mice (n=8) had a significant increase in left ventricle (LV) weight per tibia length and Fulton index compared to WT mice (n=6–7). **C)** Representative images of trichrome staining of the LV near coronary arteries of WT and SMC CYB5R3 KO mice (50-micron scalebar). Images were taken on a Tissuegnostics Microscope, stitched together using Nikon Elements Software, and analyzed using Fiji software. **D-E)** There are no significant differences in perivascular or overall cardiac fibrosis per either LV or right ventricle (RV) area between WT (n=5–6) and SMC CYB5R3 KO (n=8) mice. **F)** SMC CYB5R3 KO mice (n=8) had larger cardiomyocyte diameters in the LV, but not RV compared to WT mice (n=6–7). **G**) Wheat germ agglutinin (green) and DAPI (blue, nuclei) staining was imaged on a Nikon A1 Confocal Laser Microscope and analyzed by Nikon Elements and Fiji software (50-micron scalebar). **H**) Cardiomyocyte cross sectional area analysis showed significant differences between LV WT (n=9) and SMC CYB5R3 KO (n=7) cardiomyocytes, but not RV cardiomyocytes. The data represent mean ± standard error of

the mean (SEM). P values represent an unpaired, two tailed *t*-test and *P values represent a Mann Whitney *U* comparison of WT versus SMC CYB5R3 KO mice.

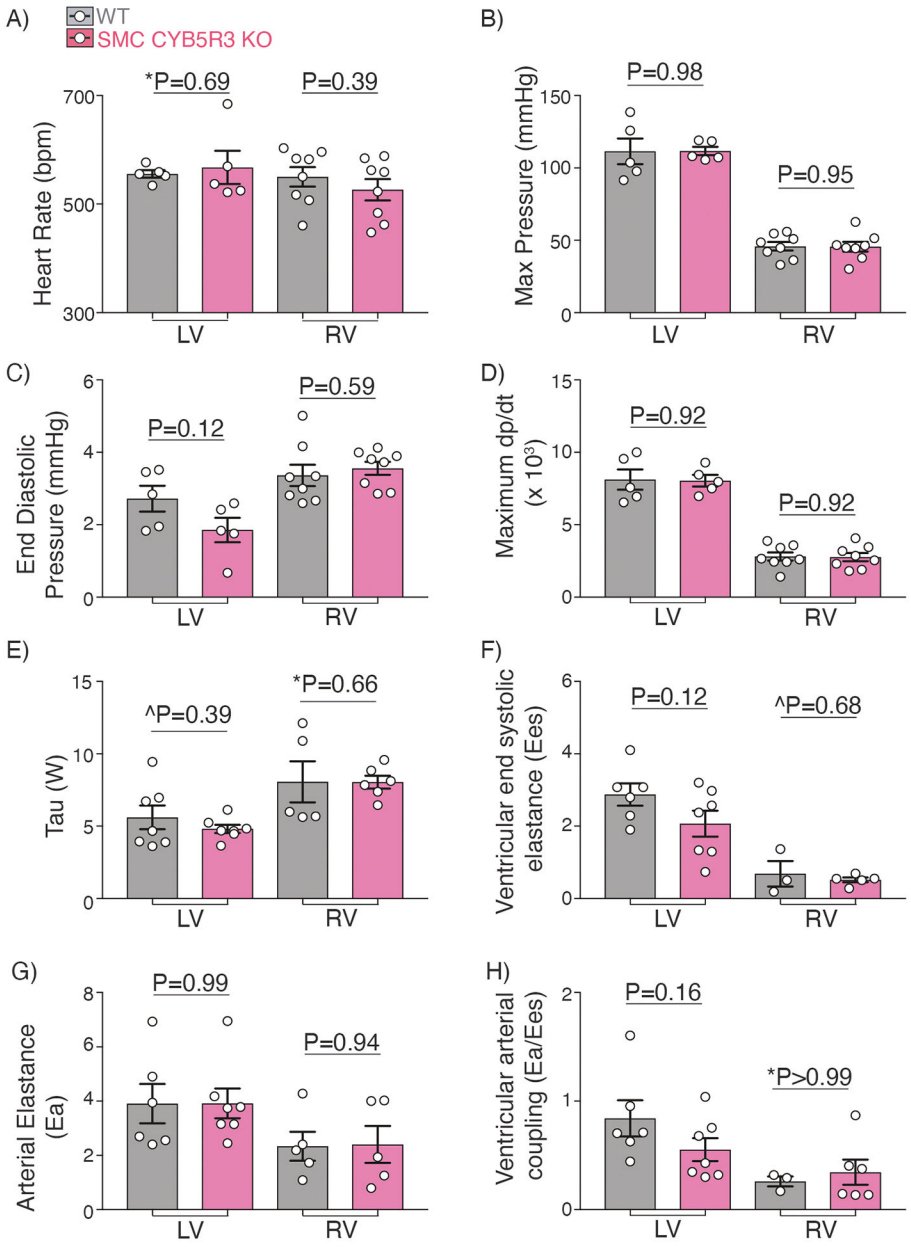

Figure 3: Chronic hypoxia treated WT and SMC CYB5R3 KO mice have similar left and right heart pressures and elastance.

Intracardiac catheterization was conducted to measure left and right heart pressures in WT and SMC CYB5R3 KO mice subjected to chronic hypoxia. **A-D)** No significant changes were seen in heart rate (bpm – beats per minute), or systolic or intracardiac pressures between WT and SMC CYB5R3 KO for either the left (n=5/group) or right (n=8/group) ventricle. **E**) Tau measurements showed no differences in either the left or right ventricle between WT (n=5–7) and SMC CYB5R3 KO mice (n=6). **F-H**) No differences were seen in ventricular end systolic elastance, arterial elastance, or ventricular arterial coupling between WT (n=3–6) and SMC CYB5R3 KO mice (n=7–5). The data represent mean ± standard error of the mean (SEM). P values represent unpaired, two tailed *t*-test comparison, ^P

represents unpaired, two tailed *t*-test comparison with Welch's correction, and *P values are Mann Whitney U comparison.

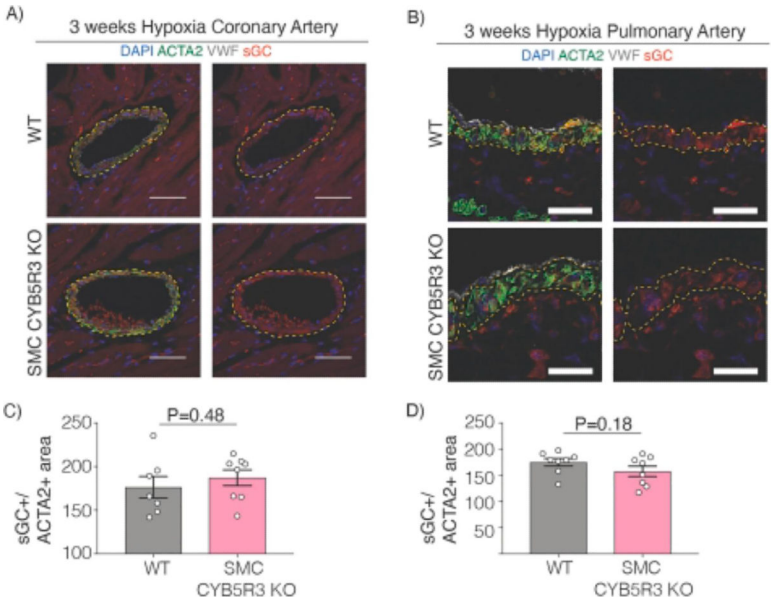

Figure 4: 3 weeks chronic hypoxia treated WT and SMC CYB5R3 KO have similar sGCβ levels in the vessel media.

Representative images of **A)** coronary arteries (50-micron scalebar) and **B)** pulmonary arteries (25-micron scalebar) of WT and SMC CYB5R3 KO mice subjected to chronic hypoxia. Images were taken on Nikon A1 Confocal Laser Microscope and analyzed by Nikon Elements and Fiji software. DAPI stains nuclei (blue). sGCβ is stained in red. ACTA2 is smooth muscle α-actin staining to delineate SMC (green). VWF is Von Willebrand Factor staining to delineate endothelial cells (gray). Yellow dashed lines highlight the boundaries of the vessel media. **C-D**) No differences in sGCβ levels per media area in coronary or pulmonary arteries were observed between WT (n=7–8) and SMC CYB5R3 KO (n=8) mice. The data represent mean ± standard error of the mean (SEM). Statistical differences were quantified by unpaired, two tailed *t*-test comparison of WT versus SMC CYB5R3 KO.

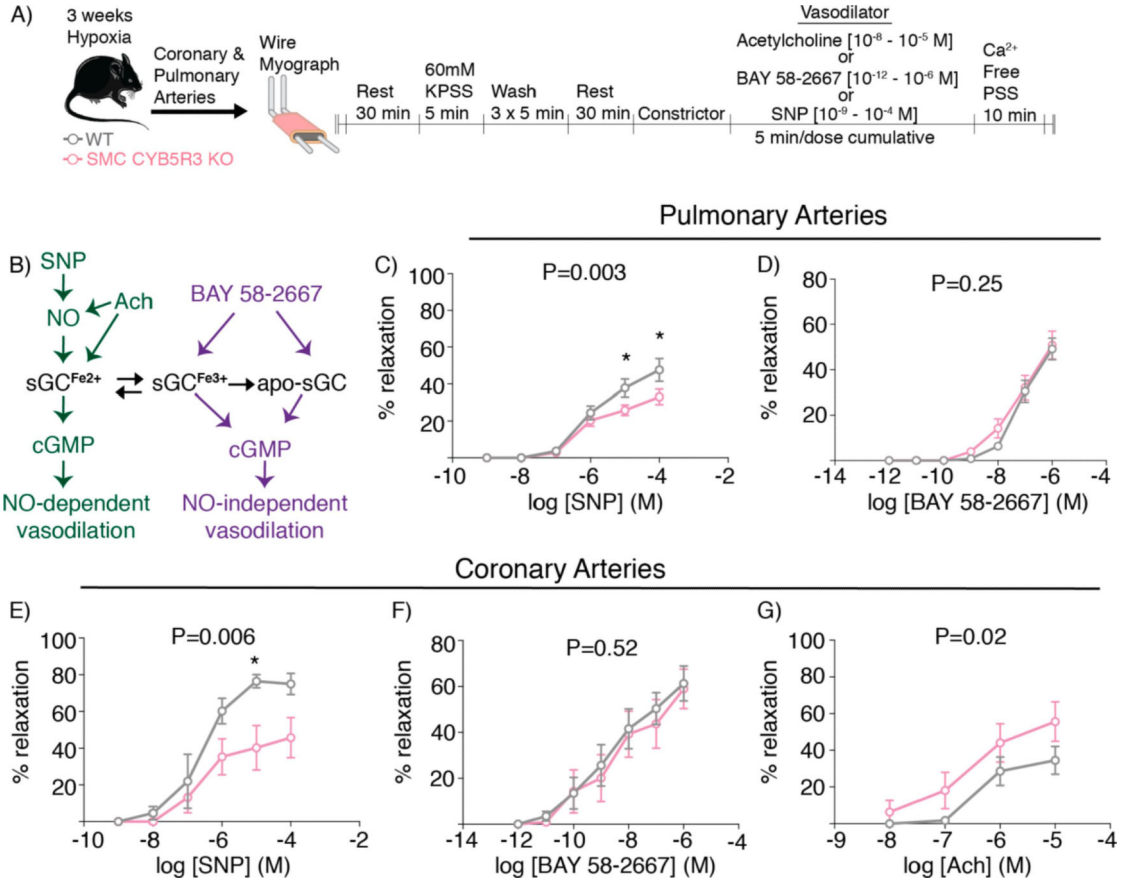

Figure 5: SMC CYB5R3 KO mice exposed to chronic hypoxia have diminished NO-dependent vasodilation compared to WT.

A) Schematic representation of the wire myography protocol. **B)** An sGC redox state schematic showing acetylcholine (Ach) and sodium nitroprusside (SNP) target the reduced (sGC^{Fe2+}) state of sGC while BAY 58–2667 targets oxidized (sGC^{Fe3+}) and/or apo-sGC to induce NO-independent vasodilation. **C-D)** Pulmonary (WT n=8; SMC CYB5R3 KO n=11) arteries of SMC CYB5R3 KO mice showed a significantly impaired NO-dependent vasodilation (SNP) but no difference in NO-independent vasodilation (BAY 58–2667) compared to WT mice. **E-F)** Similarly, coronary arteries showed SMC CYB5R3 KO mice had decreased SNP induced vasodilation compared to WT mice (n=4/group) but no significant difference in responsiveness to NO-independent BAY 58–2667 induced vasodilation (n=9–10/group). **G)** SMC CYB5R3 KO arteries (n=8) had an increased responsiveness to Ach compared to WT mice (n=7). The data represent mean ± standard error of the mean (SEM). P values represent a two-way ANOVA comparison between WT and SMC CYB5R3 KO with * representing P<0.05 by post-hoc Sidak's multiple comparisons test.